Carnegie Observatories Astrophysics Series, Vol. 4:
Origin and Evolution of the Elements, 2004
ed. A. McWilliam and M. Rauch (Pasadena: Carnegie Observatories,
http://www.ociw.edu/ociw/symposia/series/symposium4/proceedings.html)

s-Process Elements and a Lithium Substitute in Post-AGB Stars with VLT+UVES

M. REYNIERS and H. VAN WINCKEL
Institute of Astronomy, Katholieke Universiteit Leuven, Celestijnenlaan 200B, 3001 Leuven, Belgium

Abstract

Due to their high effective temperature and their relatively stable atmospheres compared to genuine AGB stars, detailed chemical studies of post-AGB stars have proven to be a very useful complement to constrain chemical evolutionary AGB models. In this contribution we describe a homogeneous study of eight s-process enriched post-AGB stars, based on high-resolution, high-S/N spectra, some of them taken with the 8.2 m VLT-UT2 (Kueyen). We will summarize the main results of this study, and discuss two important abundance relations. Another result of the new VLT data is the confirmation of the spectral line around 670.8 nm in the spectra of the enriched objects, which was interpreted in the literature as due to Li. Newly released line lists of lanthanide species reveal, however, the likely identification of the line to be due to a Ce II transition. This identification is consistent with the Ce abundance of all the enriched objects known so far.

1.1 Introduction

1.1.1 AGB Stars: What do we Expect?

The s-process that occurs in the AGB phase of low and intermediate mass stars is now qualitatively quite well understood. During the third dredge-up, both products of the He burning as well as products of the slow neutron capture (the s-process) are brought to the surface. There is now general agreement that the source of the neutrons is the "^{13}C source". The abundant carbon in the AGB inter-shell will capture a proton via the $^{12}\mathrm{C}(\mathrm{p},\gamma)^{13}\mathrm{N}(\beta^{+})^{13}\mathrm{C}$ reaction, and a significant amount of ^{13}C will be formed, the so-called ^{13}C pocket. This ^{13}C releases a neutron after an α capture: $^{13}\mathrm{C}(\alpha,\mathrm{n})^{16}\mathrm{O}$. Since this reaction requires only one α capture, it is possible at relatively low temperatures. In the older s-process models, the ^{13}C was thought to burn *during* the thermal pulse and hence in *convective* conditions. After the work of Straniero et al. (1995), it was realized that the s-process is mainly active *during* the inter-pulse phase, in *radiative* conditions.

Although the progress in the chemical evolutionary AGB models is enormous, some important issues are yet to be solved. A long standing problem is the formation of the ^{13}C pocket itself. Stellar models using a standard treatment of mixing cannot reproduce the ^{13}C pocket at a level which is high enough for the s-process to take place. The H burning has deprived the He inter-shell from protons and hence these protons have to be ingested in the inter-shell. Till now, there is no satisfying description for this phenomenon, and the different modeling groups use different descriptions. Many models use some kind of overshoot

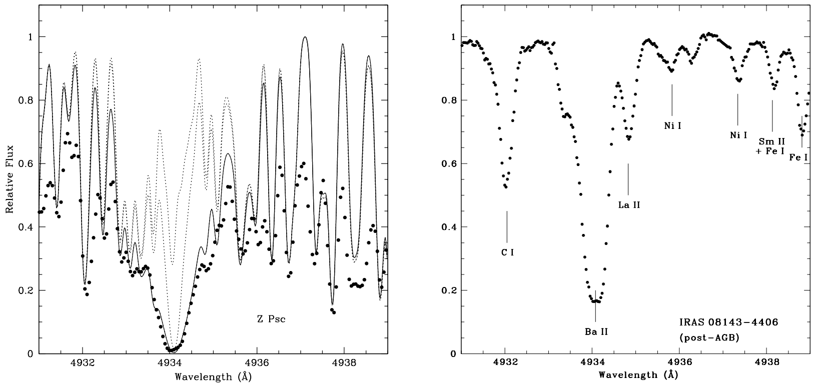

Fig. 1.1. The spectral region around the 493.408 nm resonance line of barium for an AGB star (*left*) and a post-AGB star (*right*). The spectrum of the AGB star is completely dominated by molecular lines. The full and dotted lines on the left panel are synthetic spectra with different barium abundances. It is clear that accurate abundances are extremely difficult to obtain for these stars, due to the difficult continuum placement and the overwhelming amount of molecular lines. The spectrum of the post-AGB star is mainly characterized by atomic transitions, and continuum placement is seldom a problem, except in the bluemost regions. Hence, accurate abundance determinations ($\sigma < 0.2$) are possible for these stars. (The AGB spectrum is taken from Abia et al. 2002, the post-AGB spectrum is an own VLT+UVES spectrum).

mechanism (e.g. Herwig et al. 1997). Also differential rotation has recently been studied as a possible mixing mechanism driving the proton engulfment, but this rotationally induced mixing alone cannot account for the formation of a large enough ^{13}C pocket (Herwig et al. 2003). Other groups avoid the proton engulfment problem by assuming an ad-hoc proton profile or an ad-hoc ^{13}C pocket in the He inter-shell (models by e.g. Gallino et al. 1998; Goriely & Mowlavi 2000).

1.1.2 Why to Observe Post-AGB Stars?

The observational data guiding the theoretical chemical evolutionary models come from the analysis of intrinsic AGB stars of the M-MS-S-SC-C star sequence (e.g. Lambert et al. 1995, and references therein) which is thought to reflect, at least partly, the evolution on the AGB of single stars towards an increasing C/O ratio. In addition, the enrichment in ^{12}C seems to correlate well with an increase in s-process abundances (e.g. Smith & Lambert 1990). The strong molecular opacity and sometimes unstable photospheres of AGB stars make a quantitative analysis, however, difficult and some species even untraceable. A second group of objects with excess abundances of s-process elements is the Ba star group, which is used here as a generic term for all objects for which the excess is acquired by mass-transfer from the companion which is now a white dwarf. It includes strong and mild Ba giants and Ba dwarfs, CH giant and subgiants, extrinsic S stars and since recently also yellow symbiotics (e.g. review by Jorissen 1999). The characteristics of the s-process excesses in these stars reflect the internal chemical enrichment of the companion, and the abundances may have been diluted by mixing of unprocessed material during the evolution of the gainer.

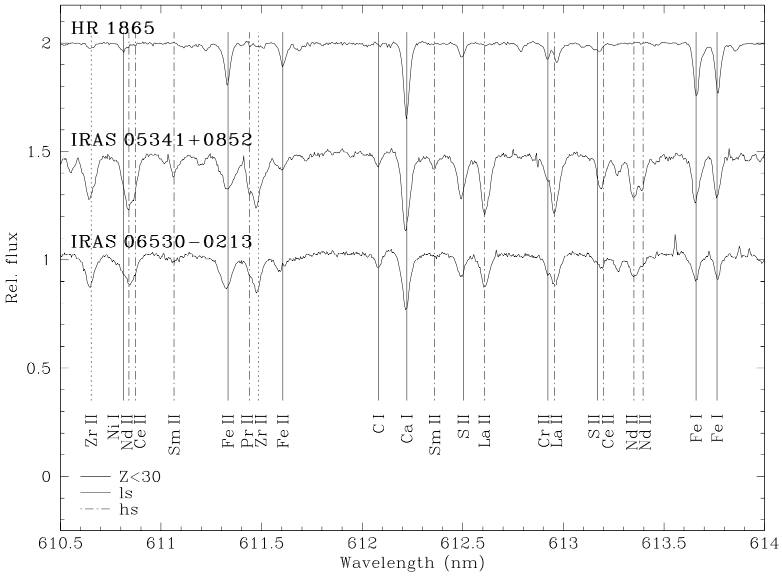

Fig. 1.2. The spectra of the s-process enriched objects IRAS 05341+0852 and IRAS 06530-0213, compared with the normal Pop. I supergiant HR 1865. The latter star has been analyzed by Decin et al. (1998) and has atmospheric parameters comparable with the other two, but with a solar metallicity. Lines of light s-process elements (Sr peak) on this figure are identified by a dotted line; lines of heavy s-process elements (Ba peak) by a dash-dotted line; lines of other elements (mainly α and iron peak elements) by a full line. The s-process enhancement of the two IRAS stars is clear. IRAS 05341+0852 is the most enriched one, but the stronger lines are also due to a slightly lower temperature of this object. All spectra are VLT+UVES spectra, except the spectrum of HR 1865, which is a WHT+UES spectrum.

Certainly for the binaries with shorter periods, the evolution (especially the mass loss) of the system might have been influenced by binary interaction.

Post-AGB stars can offer a useful complementary source of information to constrain the theoretical chemical models. Post-AGB stars are defined as stars of low and intermediate mass for which the severe mass loss at the tip of the AGB has ceased but for which the effective temperature is still too low to ionize their circumstellar environment to form a planetary nebula. While spectra of intrinsic AGB stars are dominated by molecular lines, spectra of post-AGB stars are characterized by atomic transitions (including transitions of s-process elements). This is illustrated in Fig. 1.1 in which we compare the same spectral region for an AGB and a post-AGB star. The atomic parameters of post-AGB stars allow the use of standard model atmospheres. Moreover, they show a large spread in metallicity. Unfortunately, the post-AGB phase is only a short evolutionary phase ($\sim 10^5$ yr) and hence post-AGB stars are very rare. Also, the extrapolation of results on individual objects to the whole AGB evolution theory is highly delicate: in the past, several objects that were thought to be proto-typical post-AGB stars later turned out to be rather pathological objects.

1.2 *s*-Process Enriched Post-AGB Stars

1.2.1 Observations and Spectra

In Fig. 1.2 sample spectra are shown of two s-process enriched post-AGB stars. These spectra were taken with the VLT and they nicely illustrate the quality of atomic line spectra available now. On top, the spectrum of the normal Pop I supergiant HR 1865 is shown, an object with comparable atmosphere parameters as the sample post-AGB stars (Decin et al. 1998). While the spectral lines of the α and iron peak elements are very similar for the three stars, the lines of s-process elements in the post-AGB star spectra are many times stronger than in the spectrum of the standard supergiant. It turns out that the s-process transitions dominate the spectra of the s-process enriched post-AGB stars.

The lack of molecular veiling in most post-AGB stars allows accurate abundance analyses for these objects on the base of high signal-to-noise, high resolution spectra as shown in Fig. 1.2. Since the first detection of s-process enriched post-AGB stars, numerous chemical analyses have been carried out by different groups (e.g. Klochkova 1995; Začs et al. 1995; Reddy et al. 1997, 1999, 2002; Decin et al. 1998). However, since different authors use different resolutions and different line lists, results are difficult to compare quantitatively. Therefore, a strictly homogeneous study of six s-process enriched post-AGB stars was carried out by Van Winckel & Reyniers (2000). This study has now recently been updated by Reyniers (2002). Moreover, its sample has been enlarged by two newly discovered s-process enriched objects. We will now discuss this updated study in detail. Some basic parameters of the eight objects are shown in the left part of Tab. 1.1. The instrument and spectrograph used to obtain the high resolution, high signal-to-noise spectra is also listed in this table. The three different instruments were used in approximately the same resolution.

1.2.2 Abundances

Abundances are obtained by a standard abundance analysis involving equivalent width measurement and Kurucz' model atmospheres (Kurucz 1993) in combination with the latest version of Sneden's abundance calculation program MOOG. The derived effective temperatures for the eight program stars are all between 6500 K and 8000 K, the gravities $\log g$ between 0.5 and 1.5 (cgs), and the microturbulent velocities ξ_t between 3.0 and 6.0 km s^{-1}. Errors on these quantities are typically 250 K, 0.5 (cgs), and 1 km s^{-1} respectively.

The results of our chemical analysis are graphically presented in Fig. 1.3, and an overview of the most important results is given in the right part of Tab. 1.1. On Fig. 1.3, the abundance relative to iron [el/Fe] is plotted against atomic number Z. The standard notation is used here, i.e. [el/Fe] = $\log(\mathrm{el}/\mathrm{el}_\odot) - \log(\mathrm{Fe}/\mathrm{Fe}_\odot)$. All objects display a clear and well established carbon enhancement, with [C/Fe] values lying between 0.3 and 1.1. This enrichment is beyond any doubt, even when the uncertainties of the model parameters are taken into account. The carbon enhancement is a clear indication that He burning products were brought to the surface of these objects, and that this third dredge-up was very efficient. The oxygen abundance is in most cases less certain than the carbon abundance, and only for the hotter objects a reliable oxygen abundance can be derived. Therefore, also the C/O ratio of the objects cannot be accurately obtained; the derived C/O ratios range between 1.0 to 2.8. The slight overabundances of the α-elements are expected for stars in this metallicity range: the α-elements are thus not intrinsically enhanced. The iron peak elements do follow the

Table 1.1. *Some basic parameters (left part) and summary of the main results of the homogeneous abundance study (right part) of the eight s-process enriched post-AGB stars (ls-elements are Y and Zr; hs are Ba, La, Nd and Sm; [s/Fe] is calculated with all six elements).*

IRAS	basic parameters			main abundance results			
	vis. magn. m(v)	galac. latid. b	telescope + spectrograph	[Fe/H]	[C/Fe]	[s/Fe]	[hs/ls]
04296+3429	14.2	−9.05	WHT+UES	−0.6	0.8	1.5	−0.2
05341+0852	12.8	−12.14	VLT+UVES	−0.7	1.0	2.2	0.3
06530−0213	14.1	−0.13	VLT+UVES	−0.5	1.0	2.1	0.4
07134+1005	8.3	+9.99	NTT+EMMI	−1.0	1.1	1.5	−0.1
08143−4406	12.4	−5.07	VLT+UVES	−0.4	0.5	1.5	−0.0
19500−1709	9.2	−21.04	WHT+UES	−0.7	1.0	1.2	−0.4
22223+4327	9.7	−11.56	WHT+UES	−0.3	0.3	1.1	−0.4
23304+6147	13.1	+0.59	WHT+UES	−0.8	0.9	1.6	0.1

iron deficiency, with [Fe/H] values ranging from −0.3 till −1.0, which is a strong indication that our sample indeed consists of an old and hence low-mass population.

Regarding Fig. 1.3, the overabundance of the s-process elements is beyond any doubt and is definitely the most convincing argument for the post 3rd dredge-up status of the studied stars. For unevolved objects in the same metallicity range, one expects the s-process elements to scale with Fe [el(s)/Fe] = 0.0 (e.g. Wheeler et al. 1989). Here we find overabundances of individual s-process elements up to +2.6.

The s-process elements observed in evolved stars can be divided into two groups: the light s-process elements around the magic neutron number 50 (Sr, Y, Zr) and the heavy s-process elements around the magic neutron number 82 (Ba, La, Ce, Pr, Nd, Sm, (Eu)). In order to investigate the s-process abundances in more detail, four indices are generally defined: [s/Fe], [ls/Fe], [hs/Fe] and [hs/ls]. Which elements are taken into account to determine these indices is different from author to author and is mainly determined by the possibility to compute accurate abundances of the different elements. In this contribution, we follow the proposition of Busso et al. (1995) and define the ls-index as the mean of Y and Zr and the hs-index as the mean of Ba, La, Nd and Sm. Consequently, [s/Fe] is the mean of the former six elements and [hs/ls]=[hs/Fe]−[ls/Fe]. These indices are used in Tab. 1.1 and Fig. 1.4.

1.2.3 Abundance Relations

On the left panel of Fig. 1.4 the [hs/ls] index from the eight stars is shown in comparison with the overall s-process enrichment as parameterised by the [s/Fe]-index. More objects should clearly be studied, but the total neutron exposure is surprisingly strongly correlated with the total enrichment of s-process elements, with more enriched objects showing also a stronger total neutron irradiation! A simple linear least-squares fit gives a high correlation coefficient of +0.96 with the fit $[\mathrm{hs}/\mathrm{ls}] = 0.70[\mathrm{s}/\mathrm{Fe}] - 1.14$. This correlation is, however, slightly dependent on the characterizing elements, but the final conclusion is not sensitive

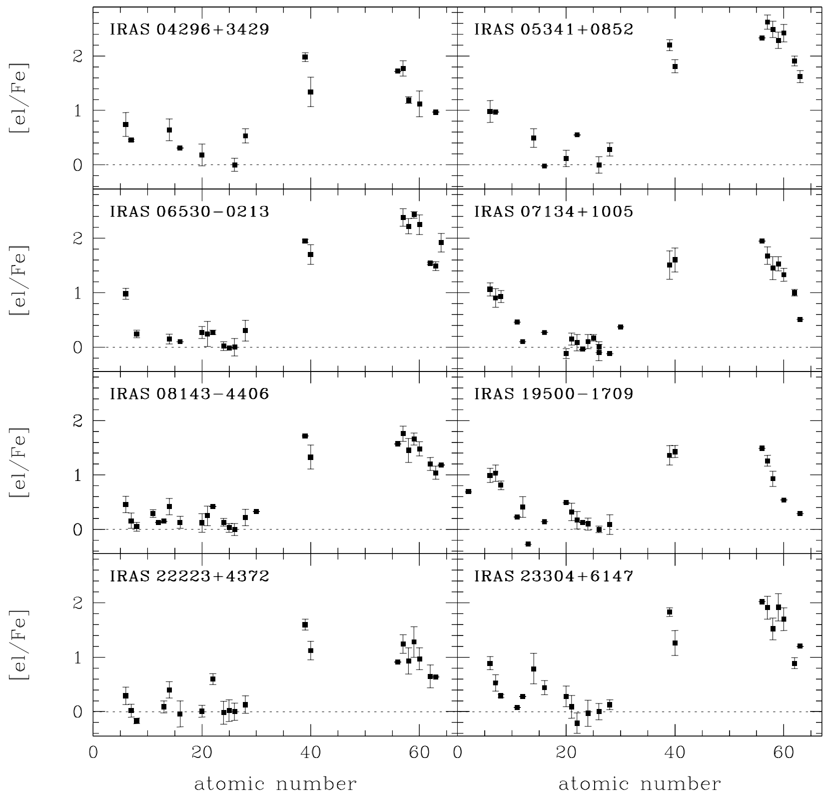

Fig. 1.3. The abundances of the eight s-process enriched post-AGB stars relative to iron [el/Fe]. The dotted line on each panel represents [el/Fe] = 0.

to the adopted species (see Reyniers 2002 for details). Since the asymptotic distribution of s-process elements is probably reached in carbon stars (Busso et al. 1995), the [hs/ls] index will not change with increasing dredge-up of enriched material in the stellar envelope, making the [hs/ls] index independent of the dilution factor of the enriched material by the initial stellar envelope material. The [hs/ls] correlation with [s/Fe] therefore reflects a different and more efficient internal nucleosynthesis, with increasing dredge-up efficiency! In AGB evolutionary models, the inclusion of protons into the inter-shell will create a primary ^{13}C pocket and induce the neutron production. Fig. 1.4 indicates therefore that, with increasing dredge-up efficiency, also the dredge-in of protons will increase, giving rise to a higher neutron irradiation.

On the right panel of Fig. 1.4, we display the [hs/ls]-index in function of the metallicity. A correlation is expected in this diagram, since in a metal deficient environment, more neutrons per iron seed are available, assuming a ^{13}C pocket independent of metallicity, and hence heavier elements can be built up in such environments. Such correlation is clearly not seen, which is also clear from the very low correlation coefficient (–0.19). For example, the strong enrichment of IRAS 06530-0213 compared to its only mild metal deficiency is a strong indication to suspect a large intrinsic spread of integrated neutron irradiations (or,

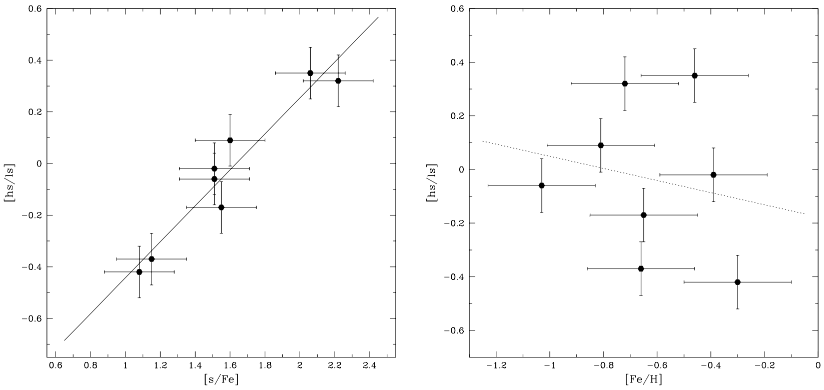

Fig. 1.4. *left panel:* The strong correlation between the total enrichment of s-process elements [s/Fe] (which is the mean of [Y/Fe], [Zr/Fe], [Ba/Fe], [La/Fe], [Nd/Fe] and [Sm/Fe]) and the [hs/ls] index. The straight line gives the simple least-squares fit. *right panel:* The [hs/ls] index as a function of the metallicity determined by the Fe abundance. The line gives the simple least-squares fit.

alternatively, ^{13}C pockets). Clearly, also other stellar parameters determine the internal AGB nucleosynthesis during the AGB evolution.

1.2.4 Elements Beyond the Ba-peak

In the two hotter objects of our sample, we detected earlier (Van Winckel & Reyniers 2000) a line of singly ionized hafnium (atomic number Z = 72). This inspired us to initiate a systematic search for s-process elements *beyond* the Ba peak in the VLT+UVES spectra of the two most heavily enriched objects in our sample (IRAS 05341+0852 and IRAS 06530-0213). Together with the widely used VALD database (Kupka et al. 1999), the recent "Database on Rare-Earths At Mons University" (http://www.umh.ac.be/∼astro/dream.shtml) lead by Prof. Biémont was an invaluable source of atomic data for this search. This work resulted in a first time detection of lines of the singly ionized species gadolinium (Z = 64), ytterbium (Z = 70), lutetium (Z = 71) and possibly also tungsten (Z = 74) in spectra of intrinsically enriched stars. Two of these detections are shown in the upper panels of Fig. 1.5. Moreover, the derived abundances of these elements are in nice agreement with their predictions in the models developed by the Torino group (lower panel of Fig. 1.5). These detections prove that also for moderate metal deficiencies, leakage from the Ba peak to the lead stability peak has occurred. Hence, the end point of the s-process (Pb) is expected to be produced, even in these moderate metal deficient objects, but unfortunately Pb has no suitable lines in the optical spectrum for these temperatures and gravities. Pb has recently been detected in extrinsically enriched stars, with a much lower metallicity (Van Eck et al. 2001).

1.2.5 Lithium in Enriched Post-AGB Stars ?

The s-process enriched post-AGB stars were claimed to be lithium rich by several authors (Začs et al. 1995; Reddy et al. 1997, 1999, 2002). The high lithium abundance was derived by the detection of a strong lithium resonance doublet. However, in all objects the

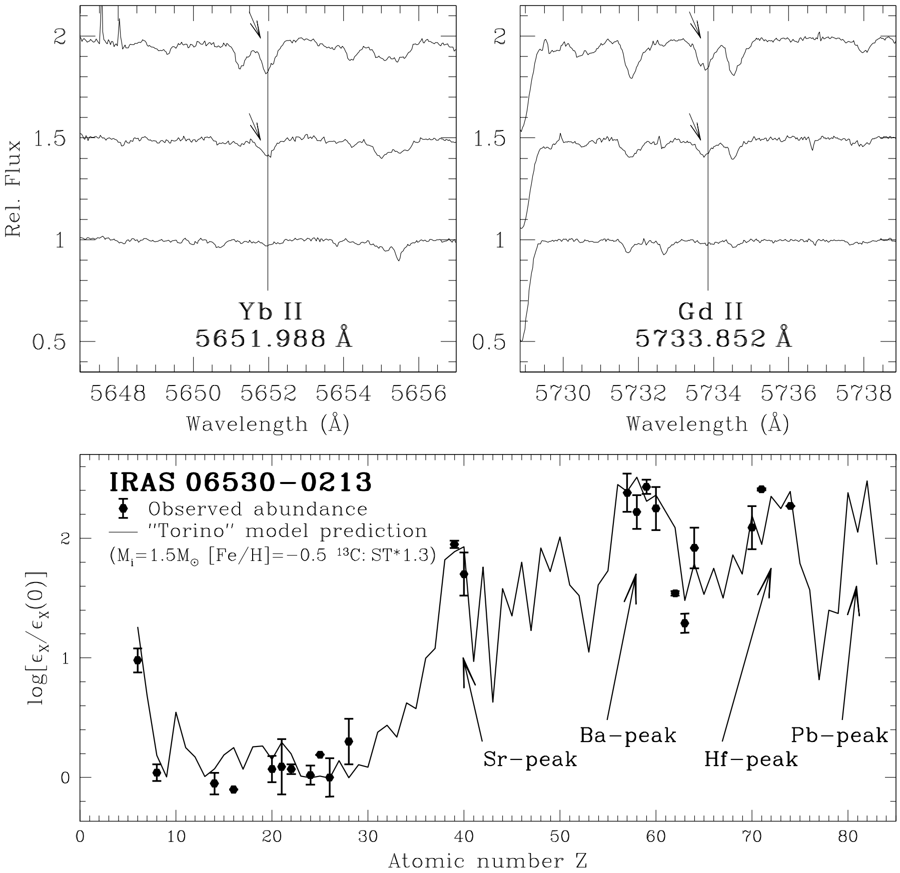

Fig. 1.5. S-process elements beyond the Ba-peak. *upper panels:* two lines of elements heavier than europium; spectra are shown of (from top to bottom) IRAS 05341+0852, IRAS 06530−0213 and IRAS 08143−4406. *lower panel:* abundances of IRAS 06530−0213 (corrected for its initial abundances) together with the best Torino model fit. The model parameters are given in the upper left corner.

doublet was shifted by 0.02 nm redward from the expected position, and a differential velocity of the Li line-forming region was invoked to explain this shift (e.g. Reddy et al. 2002). Motivated by this unexplained velocity shift of the Li-line, we investigated an alternative identification of the "shifted Li-line", which was also detected in our high signal-to-noise UVES spectra. With the use of the newly released atomic data in the D.R.E.A.M. project, we re-identified the so-called "Li-line" as a line of singly ionized cerium (Ce II) at 670.8099 nm (Reyniers et al. 2002). The Ce abundance derived from this single line is comparable to the Ce abundance derived from other Ce II lines in the spectra. Moreover, no inclusion of a significant amount of Li at photospheric wavelength was needed in a synthesis of three objects. One of these syntheses is shown in Fig. 1.6. From these results, we conclude that there is no evidence for in situ lithium production in these stars, and therefore there is no need to invoke

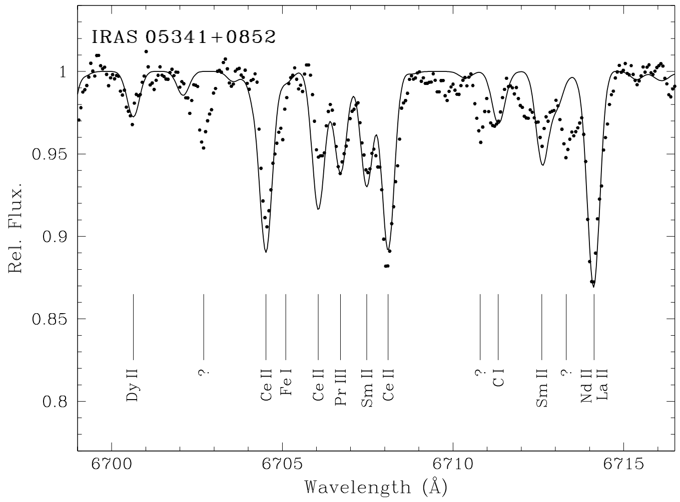

Fig. 1.6. Spectrum synthesis (full line) of the 670.8 nm region for IRAS 05341+0852 (dots). For this synthesis we used the abundances found in our abundance analysis without any modification, in order to get an idea of the quality of the line list in this region. The Li doublet was *not* included in our list. Note that there are three unidentified lines, probably from an s-process element, in this small spectral interval.

special non-standard mixing mechanisms during the AGB evolution to explain the claimed high abundances of this fragile element.

1.3 Non-enriched Post-AGB Stars

The s-process enriched post-AGB stars are only a sub-class of the whole post-AGB stellar sample. There are very similar objects (with a comparable mass and metallicity) that do not show these enhancements. This chemical dichotomy is surprisingly strict in the sense that an object is either enriched (and then it is quite severely enriched), or it is not (and then even s-process *deficiencies* are observed). This is illustrated in Fig. 1.7 on which we plotted the overabundance of the s-process element zirconium (atomic number $Z = 40$) against the metallicity for a sample of stars that all show similar characteristics for a genuine post-AGB classification, like a double peaked SED, low metallicity and kinematics. The difference is mostly directly clear from the spectrum itself. In the non-enriched objects (see e.g. Luck et al. 1990; Van Winckel 1997 for abundance analyses of these objects), no enrichments were found larger than the $[Zr/Fe] \sim 0.2$ error level. Whether this dichotomy reflects a true distribution, or is due to a selection effect, remains an open question.

1.4 Conclusions

Some post-AGB stars are among the most s-process enriched objects known so far. Thanks to their spectral type, accurate photospheric abundance studies are possible for these stars, and these studies are ideal to constrain chemical evolutionary AGB models. A homogeneous abundance study of eight s-process enriched post-AGB stars presented in this contribution reveals that we found no correlation between metallicity and s-process efficiency

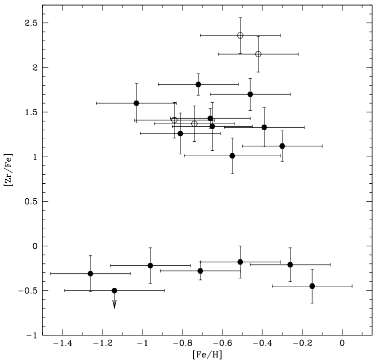

Fig. 1.7. The Zr overabundance as a function of metallicity for post-AGB stars. As can be seen from the figure, there are apparently two distinct classes: the enriched ones and the non-enriched, while these objects share a lot of other characteristics (double peaked SED, metallicity range, kinematics, etc...). Whether this dichotomy reflects a true distribution, or is due to a selection effect, remains an open question (open symbols are from Reddy et al. 1999, 2002).

(although a correlation was expected). On the other hand, we found strong correlation between dredge-up efficiency and s-process efficiency, a relation which is not a priori given by the models. In this same study, we detected lines of elements heavier than europium, which proves that also in these only moderate metal deficient objects, leakage from the Ba peak to the lead stability peak has occurred. Finally, we found that the line at 670.8 nm in s-process enriched stars is not the Li resonance line but a line of singly ionized cerium.

References

Abia, C., Domínguez, I., Gallino, R., Busso, M., Masera, S., Straniero, O., de Laverny, P., Plez, B., & Isern, J. 2002, ApJ 579, 817

Busso, M., Lambert, D. L., Beglio, L., Gallino, R., Raiteri, C. M., & Smith, V. V. 1995, ApJ 446, 775

Decin, L., Van Winckel, H., Waelkens, C., & Bakker, E. J. 1998, A&A 332, 928

Gallino, R., Arlandini, C., Busso, M., Lugaro, M., Travaglio, C., Straniero, O., Chieffi, A., & Limongi, M. 1998, ApJ 497, 388

Goriely, S., & Mowlavi, N. 2000, A&A 362, 599

Herwig, F., Bloecker, T., Schoenberner, D., & El Eid, M. 1997, A&A 324, L81

Herwig, F., Langer, N., & Lugaro, M. 2003, ApJ, 593, 1056

Jorissen, A. 1999, in IAU Symp. 191: Asymptotic Giant Branch Stars, Vol. 191, p. 437

Klochkova, V. G. 1995, MNRAS 272, 710

Kupka, F., Piskunov, N., Ryabchikova, T. A., Stempels, H. C., & Weiss, W. W. 1999, A&AS 138, 119

Kurucz, R. 1993, CD-ROM set, Cambridge, MA : Smithsonian Astrophysical Observatory

Lambert, D. L., Smith, V. V., Busso, M., Gallino, R., & Straniero, O. 1995, ApJ 450, 302

Luck, R. E., Bond, H. E., & Lambert, D. L. 1990, ApJ 357, 188

Reddy, B. E., Parthasarathy, M., Gonzalez, G., & Bakker, E. J. 1997, A&A 328, 331

Reddy, B. E., Bakker, E. J., & Hrivnak, B. J. 1999, ApJ 524, 831

Reddy, B. E., Lambert, D. L., Gonzalez, G., & Yong, D. 2002, ApJ 564, 482

Reyniers, M. 2002, PhD Thesis, Katholieke Universiteit Leuven, Belgium

Reyniers, M., Van Winckel, H., Biémont, E., & Quinet, P. 2002, A&A 395, L35

Smith, V. V., & Lambert, D. L. 1990, ApJS 72, 387

Straniero, O., Gallino, R., Busso, M., Chiefei, A., Raiteri, C. M., Limongi, M., & Salaris, M. 1995, ApJ 440, L85

Van Eck, S., Goriely, S., Jorissen, A., & Plez, B. 2001, Nature 412, 793

Van Winckel, H. 1997, A&A 319, 561

Van Winckel, H., & Reyniers, M. 2000, A&A 354, 135
Wheeler, J. C., Sneden, C., & Truran, J. W. 1989, ARA&A 27, 279
Začs, L., Klochkova, V. G., & Panchuk, V. E. 1995, MNRAS 275, 764